

Improved Irreversibility Behaviour and Critical Current Density in MgB₂-Diamond Nanocomposites

Y. Zhao^{1,2}, X.F. Rui², C.H. Cheng^{1*}, H. Zhang², P. Munroe¹, H.M. Zeng³, N. Koshizuka⁴, M. Murakami⁴

¹School of Materials Science and Engineering, University of New South Wales, Sydney 2052, NSW, Australia

²State Key Lab for Mesophysics, Department of Physics, Peking University, Beijing 100871, China

³Key Laboratory of Polymeric Composites and Functional Materials, The Ministry of Education, Zhongshan University, Guangzhou, 510275, People's Republic of China,

⁴Superconductivity Research Laboratory, ISTEK, 1-10-13 Shinonome, Koto-ku, Tokyo, 135-0062, Japan.

MgB₂-diamond nanocomposite superconductors have been synthesized by addition of nano-diamond powder. Microstructural analysis shows that the nanocomposite superconductor consists of tightly-packed MgB₂ nano-grains (~50-100 nm) with highly-dispersed and uniformly-distributed diamond nanoparticles (~10-20 nm) inside the grains. The J_c - H and H_{irr} - T characteristics have been significantly improved in this MgB₂-diamond nanocomposite, compared to MgB₂ bulk materials prepared by other techniques. Also, the J_c value of 1×10^4 A/cm² at 20 K and 4 T and the H_{irr} value of 6.4 T at 20 K have been achieved.

*Corresponding author: email: c.cheng@unsw.edu.au

Since the discovery of superconductivity at 39 K in MgB₂ [1], significant progress has been made in improving the performance of MgB₂ materials [2-4]. MgB₂ offers the possibility of wide engineering applications in the temperature range 20-30 K, where conventional superconductors, such as Nb₃Sn and Nb-Ti alloy, cannot play any roles due to their low T_c . However, the realization of large-scale applications for MgB₂-based superconductivity technology essentially relies on the improvement of the pinning behaviour of MgB₂ in high fields. As it has poor grain connection and a lack of pinning centres, MgB₂ often exhibits a rapid decrease in critical current density, J_c , in high magnetic fields. Fortunately, through the formation of nanoparticle structures in bulk MgB₂ [2-4] and thin films [5], the problem of the poor grain connection can be solved, and the flux pinning force can also be significantly enhanced due to an increase of pinning centres served by grain boundaries. In order to improve further the performance of MgB₂, it is necessary to introduce more pinning centres, especially those consisting of nano-sized second-phase inclusions, which often provide strong pinning forces.

Nano-diamond, prepared by the detonation technique, has been widely used as an additive to improve the performance of various materials [6]. Yet, nano-diamond has never been used to increase the flux pinning force in MgB₂ superconductors until the present study. The high dispersibility of the nano-diamond powder makes it possible to form a high density of nano-inclusions in MgB₂ matrix. In this letter, we have successfully prepared the MgB₂-diamond nanocomposite, which consists of tightly-packed MgB₂ nano-grains (~50-100 nm) with diamond nanoparticles (~10-20 nm) wrapped within the grains. This unique microstructure provides the composite with a good grain connection for the MgB₂ phase and a high density of flux-pinning centres served by the diamond nanoparticles. Compared to the MgB₂ bulk materials prepared with other techniques, the irreversibility line has been

significantly improved and the J_c in high magnetic fields has been largely increased in the MgB₂-diamond nanocomposite.

The MgB₂-diamond nanocomposites with compositions of MgB_{2-x}C_x (x=0, 5%, 8%, and 10%) were prepared by solid-state reaction at ambient pressure. Mg powder (99% purity, 325 meshes), amorphous B powder (99% purity, submicron-size), and nano-diamond powder (10-20 nm) were mixed and ground in air for 1 h. An extra 2% of Mg powder was added in the starting materials to compensate the loss of Mg caused by high temperature evaporation. The mixed powders were pressed into pellets with dimensions of 20x10x3 mm³ under a pressure of 800 kg/cm², sandwiched into two MgO plates, sintered in flowing Ar at 800 °C for 2 h, and then quenched to room-temperature in air. In order to compare the substitution effect of carbon in boron in MgB₂ with the additional effect of the nano-diamond in MgB₂, a sample with an added 1.5 wt% of nano-diamond in MgB₂ was prepared. The sintering temperature and the sintering time for this sample were reduced respectively to 730 °C and 30 min in order to reduce the chemical reaction between the MgB₂ and the diamond. This sample has been referred to as “1.5wt%C”.

The crystal structure was investigated by powder x-ray diffraction (XRD) using an X'pert MRD diffractometer with Cu $K\alpha$ radiation. The microstructure was analysed with a Philips CM200 field emission gun transmission electron microscope (FEGTEM). DC magnetization measurements were performed in a superconducting quantum interference device (SQUID, Quantum Design MPMS-7). J_c values were deduced from hysteresis loops using the Bean model. The values of the irreversibility field, H_{irr} , were determined from the closure of hysteresis loops with a criterion of 10² A/cm².

Figure 1 shows the XRD patterns of the nano-diamond powder and the typical MgB₂-diamond composites. The reflection (111) of the diamond is extremely broad and an amorphous-phase-like-background can be seen in the XRD pattern. The particle size of the

nano-diamond powder is estimated to be about 20 nm according to the width of the reflection. In relation to the MgB₂-diamond composites, one of the impurity phases is MgO, which may have formed during the mixing of raw materials in air. Diamond should be present as another impurity phase in the composites; however, its main reflection (111) cannot be seen in XRD patterns, due to an overlap with the MgB₂ (101) peak. As for the sample with the low doping level of x=5%, its XRD pattern looks the same as that of the undoped MgB₂, except for a decrease of the lattice parameter along the *a*-axis, indicating that a certain amount of carbon atoms have substituted for boron atoms in MgB₂. This result is consistent with those reported by other groups, which show that partial substitution of boron by carbon results in a decrease of the lattice parameter [7,8]. With increasing doping level, an amorphous-phase-like background in the XRD pattern gradually appears, suggesting the existence of unreacted nano-diamond in the sample. As for the diamond-added MgB₂ sample (1.5wt%C), which contains an x=5.4% equivalent percentage of carbon atoms, the background of its XRD pattern shows some similarity to the background of the nano-diamond, suggesting that a substantial amount of unreacted nano-diamond exists within this sample.

The substitution of boron by carbon in our MgB₂ can also be reflected by the gradual decrease of T_c with increasing carbon content (see the inset of Fig.2). The values of onset T_c for these carbon-substituted MgB₂ samples are 38.6 K for x=0, 36.1 K for x=5%, 33.0 K for x=8%, and 31.3 K for x=10%. The T_c for the sample 1.5wt%C is 36.9 K, which is higher than that for the sample of x=5% (T_c =36.1 K), despite the former having a higher equivalent atomic percentage of carbon (x=5.4%).

Figure 2 shows the magnetic field dependence of J_c at 10, 20, and 30 K for the carbon-substituted MgB₂ samples. At 30 K, the undoped MgB₂ exhibits the highest J_c and the slowest decrease of J_c with H ; whereas the sample of x=10% shows the lowest J_c and the quickest drop of J_c with H . It is evident that the J_c - H behaviour at 30 K for these samples is positively

correlated to their T_c values. However, when the temperature decreases to the values far below T_c , a totally different situation appears. For example, at 10 K and 20 K, the diamond-doped samples show a much better J_c - H behaviour. The J_c drops much more slowly in diamond-doped samples than in pure MgB_2 . The best J_c at 20 K is found in the sample of $x=10\%$, reaching a value of $6 \times 10^3 \text{ A/cm}^2$ in a 4 T field, indicating that a strong flux pinning force exists in these diamond-doped samples.

The $H_{\text{irr}}-T$ relations for the diamond-substituted MgB_2 are shown in the inset of figure 3. The $H_{\text{irr}}(T)$ curves get steeper with increasing doping level. The best value of H_{irr} reaches 5.7 T at 20 K for the sample of $x=10\%$. As the T_c values vary with the diamond-doping level, only the $H_{\text{irr}}-T$ relation cannot directly reflect the intrinsic irreversibility behaviour for the samples of different doping levels. In the main panel of Fig.3, the temperature dependence of H_{irr} is replotted using a reduced temperature, T/T_c . It is evident that the irreversibility field shifts towards higher temperatures with the increase of the diamond-doping level. The result clearly shows that the diamond doping does enhance the flux pinning in MgB_2 significantly.

However, the effect of diamond doping on the enhancement of flux pinning in MgB_2 may be counterbalanced by its suppression on superconductivity, as clearly shown in the situation of $T=30 \text{ K}$ (see Fig.2). This counterbalancing effect may also exist at other temperatures, even when the effect of the J_c -enhancement is dominant. The further increase of J_c depends critically on reducing the T_c -suppression effect in the MgB_2 -diamond composite. This idea is confirmed by the results obtained in the diamond-added sample, 1.5wt%C, which has a higher T_c than other diamond-doped samples (see inset of Fig.2) and contains more nano-diamond inclusions as suggested by the XRD analysis (see Fig.1) and confirmed by our TEM analysis shown below. As shown in figure 4, the diamond-added sample shows a much better J_c - H behaviour than the carbon-substituted sample. Its J_c reaches $1 \times 10^4 \text{ A/cm}^2$ at 20 K and 4 T, and its H_{irr} reaches 6.4 T at 20 K. In fact, at all temperatures below 35 K, the J_c - H

behaviour (results at 20 K are shown here only) and the H_{irr} - T relation (see the inset of Fig.4) of the diamond-added sample are much better than those of other samples in this study.

Fig.5 shows the typical results from microstructural analysis for the diamond-substituted MgB₂ and diamond-added MgB₂ samples. The diamond-substitutional sample mainly consists of relatively large MgB₂ grains (~1 micron or so in size) with a high density of dislocations. In some areas, discrete nano-sized particles can be seen (Fig.5a). The diamond-added sample mainly consists of two kinds of nanoparticles: MgB₂ grains with a size of 50-100 nm and diamond particles with a size of 10-20 nm (see Fig.5b). In fact, this diamond-added MgB₂ forms a typical nanocomposite material. The nano-diamond particles are inserted into the MgB₂ grains. As the *ab*-plane coherence length of MgB₂ is about 6-7 nm [9], these 10- to 20-nm-sized diamond inclusions, with a high density, are ideal flux pinning centres and are responsible for the high performance in our samples.

It is worth noting that the enhancement of flux pinning in nano-diamond-doped MgB₂ is even better than the Ti-doped MgB₂ [2-4], where the TiB₂ nanoparticles mainly stay in grain boundaries. This suggests that a highly dispersed distribution of nano-inclusions in MgB₂ is more effective in enhancing flux pinning than a more localised distribution in the grain boundaries. Besides, compared to the Y₂O₃ nano-particle doping, an advantage of the nano-diamond doping is that the lattice contact of the cubic diamond ($a=0.356$ nm) is very close to the *c*-axis of MgB₂ ($c=0.352$ nm). Therefore, these diamond nanoparticles may provide nucleation centres for MgB₂ and are tightly bound to them. This may explain why our MgB₂-diamond nanocomposite performs much better than the nano-Y₂O₃-doped MgB₂ [10]. It is expected that the performance of the MgB₂-diamond nanocomposite may be further improved by optimising the microstructure and the doping levels.

In summary, we have successfully synthesized a MgB₂-diamond nanocomposite superconductor by adding nano-diamond powder into MgB₂. The nanocomposite consists of

tightly-packed MgB₂ nano-grains (~50-100 nm) with diamond nanoparticles (~10-20 nm) inserted inside these grains. The J_c - H and H_{irr} - T characteristics have been significantly improved in this MgB₂-diamond nanocomposite, in comparison with MgB₂ bulk materials prepared with other techniques.

Acknowledgement The authors are grateful to Miss Sisi Zhao for her helpful discussion in preparing the manuscript. This work was supported in part by the University of New South Wales (Goldstar Award for Cheng). Financial support from the Ministry of Science and Technology of China (NKBRFSF-G19990646) is also acknowledged.

References:

1. J. Nagamatsu, N. Nakagawa, T. Muranaka, Y. Zenitani, J. Akimitsu, *Nature* **410**, 63 (2001).
2. Y. Zhao, Y. Feng, C.H. Cheng, L. Zhou, Y. Wu, T. Machi, Y. Fudamoto, N. Koshizuka, and M. Murakami, *Appl. Phys. Lett.* . **79** 1154 (2001).
3. Y. Zhao, D.X. Huang, Y. Feng, C.H. Cheng, T. Machi, N. Koshizuka, and M. Murakami, *Appl. Phys. Lett.* **80**, 1640 (2002).
4. Y. Zhao, Y. Feng, T. Machi, C.H. Cheng, D.X. Huang, Y. Fudamoto, N. Koshizuka, and M. Murakami, *Europhys. Lett.* **57**, 437 (2002).
5. C.B. Eorn, M.K. Lee, J.H. Choi, L.J. Belenky, X. Song, L.D. Cooley, M.T. Maus, S. Patnaik, J. Jiang, M. Rikel, A. Polyanskii, A. Gurevich, X.Y. Cai, S.D. Bu, S.E. Babcock, E.E. Hellstrom, D.C. Larbalestier, N. Rogado, K.A. Regan, M.A. Hayward, T. He, J.S. Slusky, K. Inumaru, M.K. Haas, and R.J. Cava, *Nature*, **411**, 558 (2001).
6. Q. Chen and S. Yun, *Mater. Res. Bull.* **35**, 1915 (2000).
7. T. Takenobu, T. Ito, D.H. Chi, K. Prassides, and Y. Iwasa, *Phys. Rev. B* **64**, 134513 (2001).
8. W. Mickelson, J. Cumings, W.Q. Han, and A. Zettl, *Phys. Rev. B* **65**, 052505 (2002).
9. M. Xu, H. Kitazawa, Y. Takano, J. Ye, K. Nishida, H. Abe, A. Matsushita, N. Tsujii, G. Kido. *Appl. Phys. Lett.*, **79**, 2779 (2001).
10. J. Wang, Y. Bugoslavsky, A. Berenov, L. Cowey, A.D. Caplin, L.F. Cohen, J.L. MacManus Driscoll, L.D. Cooley, X. Song, and D.C. Larbalestier, *Appl. Phys. Lett.* **81**, 2026 (2002).

Figure Captions:

Figure 1 Powder XRD patterns for MgB₂-diamond nano-composites. The pattern on the top row is for the nano-diamond.

Figure 2 Magnetic field dependence of J_c at 10, 20, and 30 K for MgB_{2-x}C_x with x=0 (dashed lines), 5% (solid lines), 8% (solid circles), and 10% (opened triangles). Inset: superconducting transition curves for the diamond-doped samples. The closed circles represent the results for the sample 1.5wt%C.

Figure 3 Variation of H_{irr} with reduced temperature T/T_c for MgB_{2-x}C_x with x=0, 5%, 8%, and 10%. Inset: $H_{irr}-T$ plot for the same data shown in the main figure.

Figure 4 Comparison of J_c-H relations at 20 K for diamond-added MgB₂ sample 1.5wt%C with diamond-substituted MgB₂. The atomic percentages of carbon in the sample 1.5wt%C and the sample of x=5% are almost the same. Inset: $H_{irr}-T$ relations for the same samples shown in the main figure.

Figure 5 FEGTEM micrographs for (a) diamond-substituted MgB₂ with x=5%; (b) diamond-added MgB₂ with the carbon content of 1.5 wt%. The atomic percentages of carbon in these two samples are almost the same.

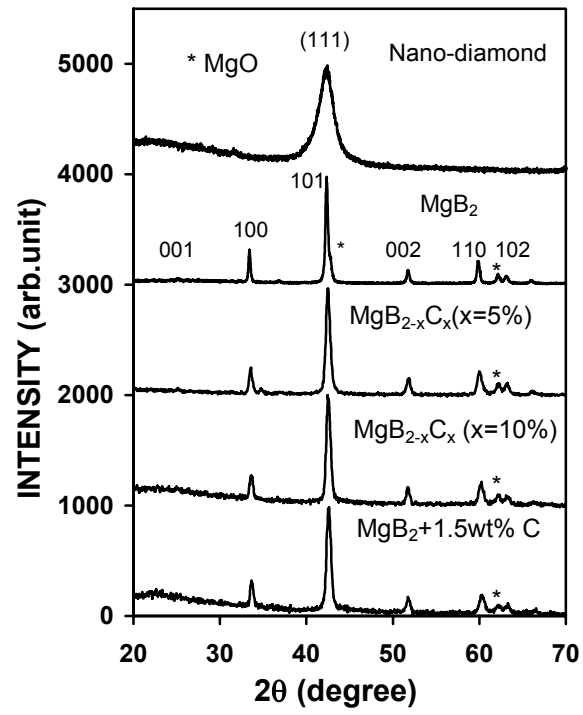


Fig.1

Y. Zhao et al.

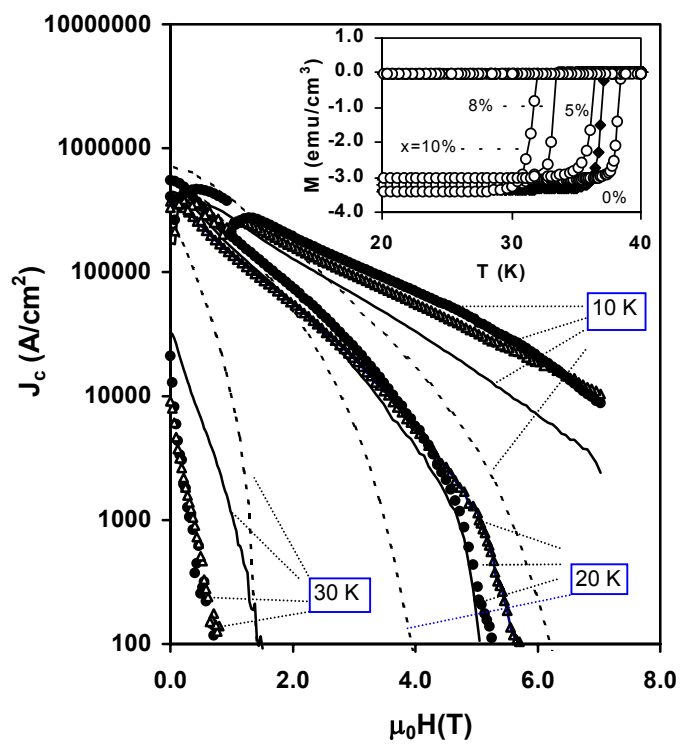


Fig. 2

Y. Zhao et al

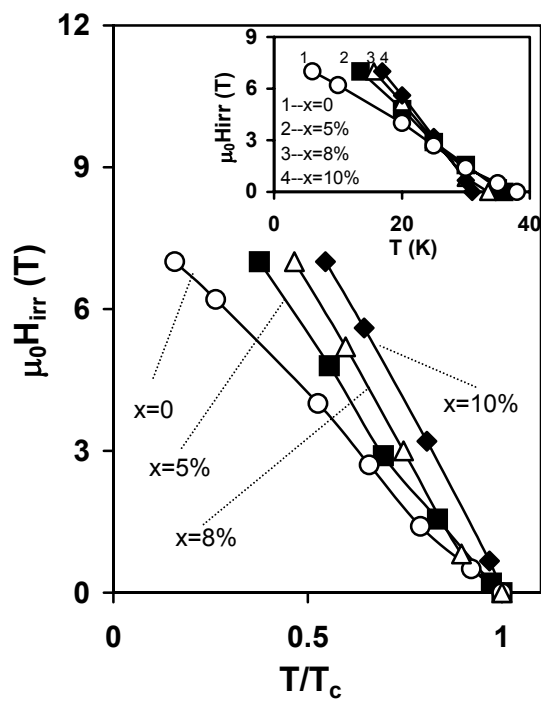


Fig.3

Y. Zhao et al

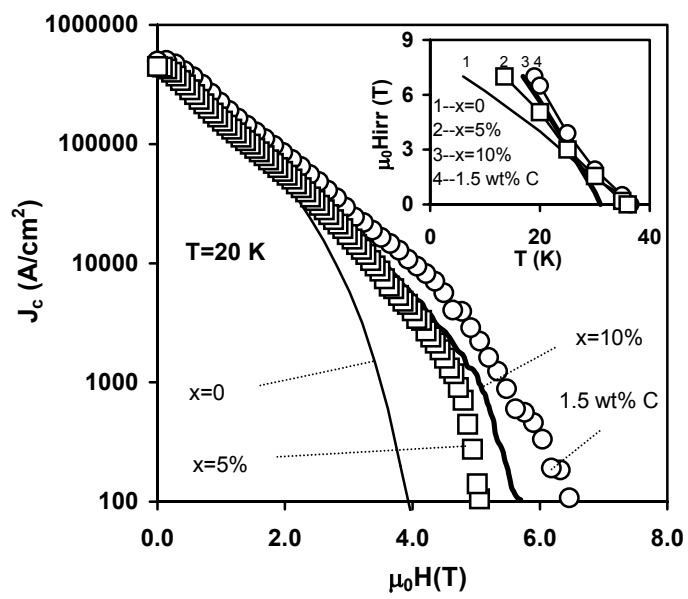


Fig.4

Y. Zhao et al

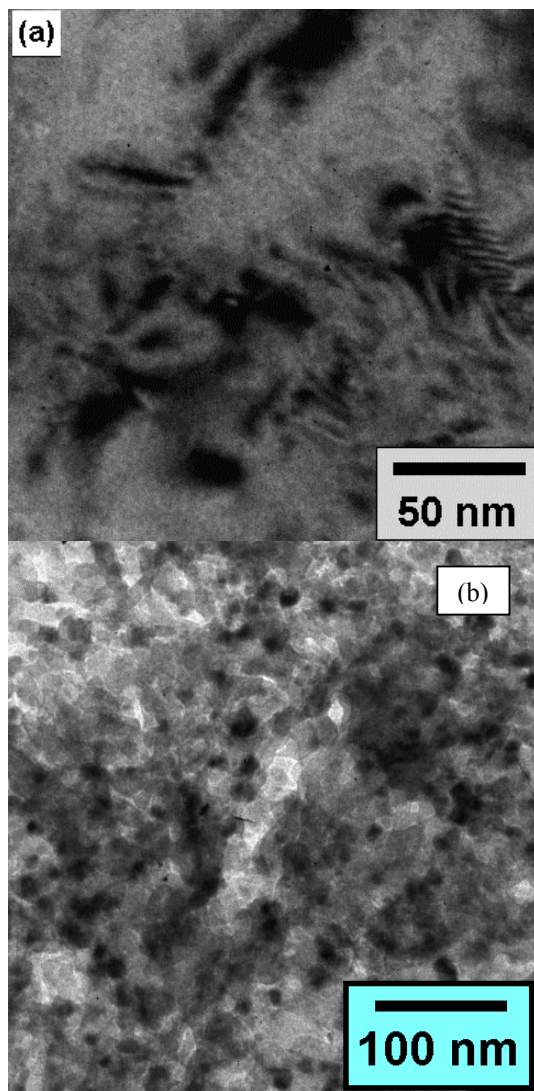


Fig. 5

Y. Zhao et al